Original article

Size and time-dependent induction of proinflammatory cytokines expression in brains of mice treated with gold nanoparticles

Haseeb A. Khan [a], Salman Alamery [a,b], Khalid E. Ibrahim [c], Doaa M. El-Nagar [d], Najla Al-Harbi [a], Mohamad Rusop [e], Salman H. Alrokayan [a,*]

[a] Department of Biochemistry, College of Science, King Saud University, Riyadh, Saudi Arabia
[b] Center of Excellence in Biotechnology Research, College of Science, King Saud University, Riyadh, Saudi Arabia
[c] Department of Zoology, College of Science, King Saud University, Riyadh, Saudi Arabia
[d] Department of Zoology, College of Girls for Science, Arts and Education, Ain Shams University, Cairo, Egypt
[e] NANO-Electronic Centre, Faculty of Electrical Engineering, Universiti Teknologi MARA, Shah Alam, Selangor, Malaysia

ARTICLE INFO

ABSTRACT

Gold nanoparticles (GNPs) are among the ideal nano-sized materials for medical applications such as imaging and drug delivery. Considering the significance of recent reports on acute phase induction of inflammatory mediators by GNPs, we studied the effect of GNPs on proinflammatory cytokines gene expression in mouse brain. Group 1 served as control whereas groups 2–4 were given only one intraperitoneal dose of 5, 20 and 50 nm GNPs, respectively and sacrificed after 24 h. The animals in groups 5–7 also received the same treatment but sacrificed after 7 days. Groups 8–10 received two injections of GNPs (5, 20 and 50 nm, respectively), first at the beginning of study and second on day 6, and sacrificed on day 7. Total RNA was extracted from the cerebral tissue and analyzed for the gene expressions of IL-1β, IL-6 and TNF-α. A single injection of 5 nm diameter GNPs significantly increased the mRNA expression of IL-1β and IL-6 in mouse brain on day 7, which was not augmented by the second dose of the same GNPs. Larger size GNPs (20 nm and 50 nm) did not cause any significant change in the expression of proinflammatory cytokines in mouse brain. In conclusion, systemic administration of small sized GNPs (5 nm) induced a proinflammatory cascade in mouse brain indicating a crucial role of GNPs size on immune response. It is important to use the right sized GNPs in order to avoid an acute phase inflammatory response that could be cytotoxic or interfere with the bioavailability of nanomaterials.

© 2018 The Authors. Production and hosting by Elsevier B.V. on behalf of King Saud University. This is an open access article under the CC BY-NC-ND license (http://creativecommons.org/licenses/by-nc-nd/4.0/).

1. Introduction

Engineered nanoparticles (NPs) have multifaceted industrial and biomedical applications in various fields such as cosmetic, paint, and food industry, electronics, disease diagnosis and therapy (Nafiujjaman et al., 2017, 2015; Salifairus et al., 2016; Kang et al., 2015; Khatun et al., 2015; Nurunnabi et al., 2015; Eswar et al., 2014). Owing to their robust nature, ease of functionalization, excellent biocompatibility and optical properties, gold nanoparticles (GNPs) have emerged as preferential candidates for drug delivery, therapy and imaging applications (Falagan-Lotsch et al., 2016; Calderón-Gonzalez et al., 2016). After the discovery that GNPs have the ability to cross the blood brain barrier (BBB), they are being thoroughly investigated for diagnostic imaging and therapy of neurological disorders including brain tumor. The BBB controls the brain microenvironment by limiting the entry of unwanted chemicals into the central nervous system (CNS) thereby creating an obstacle for many medical therapeutic and imaging procedures.

Exposure to GNPs increased endothelial paracellular permeability in-vitro and elevated BBB permeability in-vivo (Li et al., 2015). Trafficking of GNPs coated with specific receptor antibody has been used for receptor-mediated transcytosis to ensure the transport of neurotherapeutics across the BBB (Cabezón et al., 2015). Betzer et al. (2017) synthesized 20, 50 and 70 nm insulin-coated gold nanoparticles (INS-GNPs) and tested their ability to cross the BBB in mice. The highest accumulation in brain was observed using INS-GNPs (20 nm), 2 h after injection. The CT imaging showed that

nanoparticles migrated to specific brain regions which are associated with neuropsychiatric and neurodegenerative disorders, suggesting the possible application of INS-GNPs in delivering potential treatments for brain diseases (Betzer et al., 2017). Intramuscularly injected drug-conjugated GNPs crossed the BBB and delivered the drug into the brain stem and spinal cord of rats for the treatment of respiratory muscle paralysis due to cervical spinal cord injury (Zhang et al., 2016). Compared with citrate GNPs, the amphipathic peptide (CLPFFD)-conjugated GNPs improved (4-fold increase in gold concentration), while the conjugate was partly washed out from the brain but mainly accumulated in the liver after 24 h (Guerrero et al., 2010). Further modification of CLPFFD-conjugated GNPs with another peptide sequence (THRPPMWSPVWP) that interacts with the transferrin receptor present in the microvascular endothelial cells of the BBB has been shown to increase the permeability of the conjugated GNPs in brain. This strategy has been tested to destroy the toxic aggregates of β-amyloid, similar to that found in the brains of Alzheimer's disease patients (Prades et al., 2012).

Small sized GNPs coated with gadolinium chelates can be traced by MRI after intravenous injection for accurate radiosensitization to improve the selectivity and efficiency of brain tumor radiotherapy (Miladi et al., 2014). Meyers et al. (2015) have reported epidermal growth factor peptide-targeted GNPs as a novel approach for targeted delivery and photodynamic therapy of brain cancer. Ruan et al. (2015) functionalized PEG-coated and doxorubicin-loaded GNPs with angiopep-2, a specific ligand of low density lipoprotein receptor-related protein-1, which mediated the system to penetrate BBB and specifically delivered and released doxorubicin in glioma and enhanced the survival of mice. A single intravenous injection of peptide-modified 5 nm GNPs efficiently crossed the BBB and delivered the anticancer drug doxorubicin as well as the contrast agent gadolinium for the treatment and imaging of brain tumor in mice (Cheng et al., 2014). Brain tumor bearing mice receiving 11 nm GNPs and radiation (30 Gy) showed that GNPs uptake of 19:1 tumor to normal brain ratio that increased local radiation dose by approximately 300% resulting in 50% long term survival as compared to 100% mortality in mice receiving radiation only (Hainfeld et al., 2013). Bobyk et al. (2013) determined the efficiency of gold photoactivation by intracerebral infusion of GNPs followed by irradiation of rat glioma. The rats receiving the combined treatment (GNPs + 15 Gy) lived longer than those animals that were treated with the radiation alone.

The above literature clearly indicates the wider scope of GNPs in imaging and therapy of neurological diseases. However, there is still limited information available about the toxicity of GNPs to neural tissue. A thorough characterization of nanomaterials is important to understand any associated adverse effects and to ensure their safe applications (Khan and Shanker, 2015). Earlier studies have reported GNPs-induced alterations in proinflammatory cytokines expression in liver and kidneys of rats (Khan et al., 2013a, 2013b, 2016, 2017). However, the impact of GNP exposure on induction of inflammatory mediators in brain was never investigated. By virtue of their direct interaction with serum proteins (including opsonins), naked GNPs have a higher rate of cellular uptake whereas conjugation of GNPs with materials such as polyethylene glycol can significantly reduce their surface interactions and thus cellular uptake (Chithrani and Chan, 2007). In this investigation, we studied the effects of naked GNPs (5, 20 and 50 nm diameter) on mRNA expressions of proinflammatory cytokines including IL-1β, IL-6 and TNF-α in mouse brain.

2. Materials and methods

2.1. Animals and treatment groups

Adult Swiss albino mice weighing 25–35 g were used in this study. The mice were kept in polycarbonate cages with sawdust bedding and housed in an air-conditioned room with proper day/night cycle. The mice were provided with the normal chow food and water ad libitum. Mice were divided into 10 treatment groups of 6 animals in each group. Group 1 was treated with vehicle only and this group served as control group. The animals in groups 2–4 were treated with a single intraperitoneal injection of 5, 20 and 50 nm GNPs, respectively and sacrificed after 24 h. The animals in groups 5–7 also received the same treatment but sacrificed after 7 days. Groups 8–10 received two injections of GNPs (5, 20 and 50 nm, respectively), first injection at the beginning of study and second on day 6, and sacrificed on day 7. The experimental segments are summarized in Fig. 1.

2.2. Gold nanoparticles

Gold nanoparticles of 5 nm, 20 nm and 50 nm diameter (Au concentration of 0.01%) were obtained from MK Impex Corp., Canada. The working dilutions of GNPs were stored at 2–8 °C. The dimensions and morphological appearance of GNPs were tested by transmission electron microscopy (TEM) and shown in Fig. 2. The GNPs of 5 nm and 20 nm diameter appeared to be round whereas the GNPs of 50 nm size were found to be hexagonal in shape (Fig. 2).

2.3. Animal dosing

The stock solutions of different size GNPs (5, 20 and 50 nm) were diluted with normal saline and administered intraperitoneally in the volume of 100 μl for each animal. This dosage
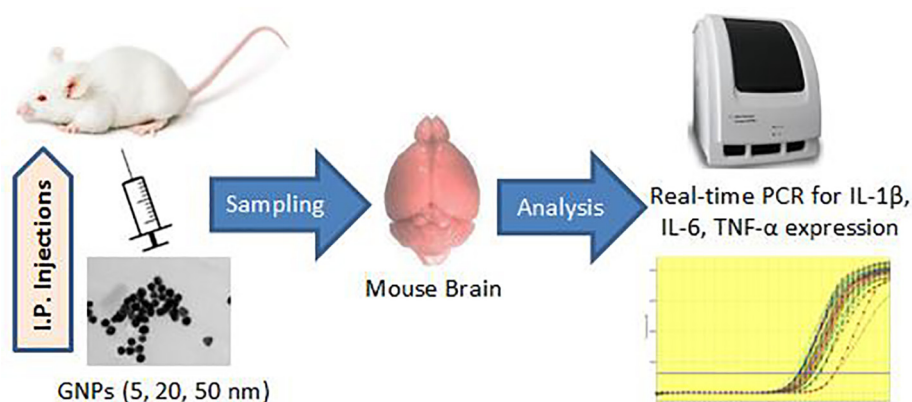
Fig. 1. Simplified layout of experimental protocol.
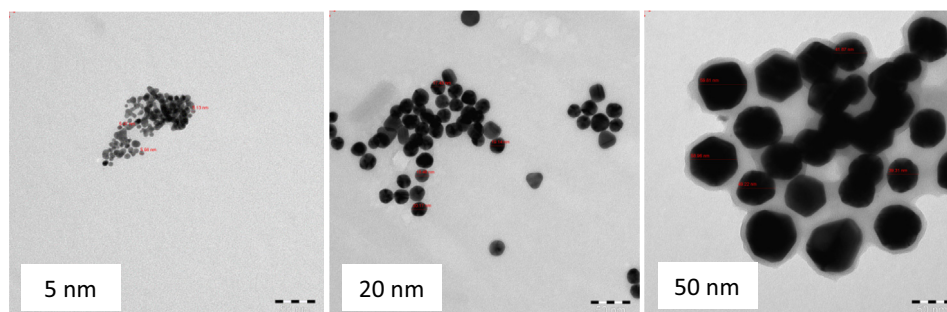
Fig. 2. Transmission electron microscopy for determining the size and shape of GNPs. Scale bar = 50 nm.

corresponds to 5 μg Au/mouse and equivalent to around 170 μg/kg bodyweight. As mentioned above, there was a control group and three sets of GNP-treated groups to study the effects of a single injection of 5, 20 and 50 nm GNPs after day 1 (Groups 2–4) and day 7 (Group 5–7) as well as two injections of GNPs (6 days apart) and sacrificed on day 7 (Groups 8–10, priming dose groups).

The mice were sacrificed 24 h after a single injection (Groups 2–4), 7 days after a single injection (Groups 5–7) and 24 h after second injection (Groups 8–10). The brains were removed and immediately dipped in RNAlater solution (Qiagen, USA) and immediately kept at 4 °C until the extraction of RNA was performed. The study protocol was approved by the Institutional Ethics Board.

2.4. Real-time PCR analysis

Total RNA was isolated from about 30 mg of pre-stabilized cerebral tissues using SV total RNA Isolation System (Promega Corporation, USA), according to manufacturer's guidelines. The RNA was finally dissolved in 100 μl of nuclease free distilled water and stored at −80 °C. The purity and concentration of RNA samples were measured by a Nanodrop Spectrophotometer (Thermo Fisher Scientific, USA). The ImProm-II Reverse Transcription System (Promega Corporation, USA) was used for reverse transcription cDNA synthesis according to manufacturer's instructions.

Real-time PCR reaction was carried out in a 25 μl reacting mixture containing 0.5 μl of each primer, 1.5 μl of cDNA and 13 μl SYBR Green real-time PCR Master Mix (Qiagen, USA). Each run consisted of an initial denaturation step at 95 °C for 5 min followed by 45 cycles of 95 °C for 30 s, 60 °C for 10 s, and 72 °C for 10 s followed by melting curve analysis in a real-time PCR instrument (Stratagene, Agilent, USA). A housekeeping gene (β-actin) was used for normalizing the gene expression data. The sequences of primers used in this study are given in Table 1.

2.5. Statistics

The data were first subjected to one-way analysis of variance (ANOVA) and then tested with Dunnett's test using SPSS software. The statistical significance was set at $P < 0.05$.

Table 1
Primers used for real-time PCR amplifications.

Primer name	Sequence	Base pairs
Mouse IL-1β-F	GCTCATCTGGGATCCTCTCC	20
Mouse IL-1β-R	CCTGCCTGAAGCTCTTGTTG	20
Mouse IL-6-F	CTTGGGACTGATGCTGGTGA	20
Mouse IL-6-R	TGCAAGTGCATCATCGTTGT	20
Mouse TNF-α-F	ACCCCCTGAGTCTGCTCAAT	20
Mouse TNF-α-R	CCTGGTGGGACTTGGTTGTA	20
Mouse β-Actin-F	CTGGTCGTACCACAGGCATT	20
Mouse β-Actin-R	CTCTTTGATGTCACGCACGA	20

3. Results

Administration of a single dose of GNPs of different sizes (5 nm, 20 nm, 50 nm) caused slight reductions in the mRNA expression of IL-1β on day 1 whereas GNPs of 5 nm diameter significantly increased IL-1β expression on day 7 (ANOVA F = 5.082, P = 0.001) (Fig. 3, upper panel). The second injection of GNPs after one week did not exacerbate the effects of GNPs on brain IL-1β (Fig. 3). Although brain IL-6 mRNA expression on day 1 was not affected by GNPs of different sizes, it was significantly increased by small sized GNPs (5 nm) on day 7 post-dosing (ANOVA F = 2.089, P = 0.049) (Fig. 3, middle panel). The primed animals (two doses six days apart) did not show any further increase in IL-6 gene expression after the second dose of GNPs. The expression of TNF-α in mouse brain was unaffected by GNPs irrespective of their sizes or dose regimens (ANOVA F = 0.465, P = 0.891) (Fig. 3, lower panel).

The real-time PCR amplification plots and respective melting curves for IL-1β, IL-6 and TNF-α are shown in Fig. 4. The average count of threshold cycle (Ct) for the house keeping gene β-actin was 18.47. The average counts of Ct for the target genes were as follows: IL-1β (Ct = 29.46), IL-6 (Ct = 31.54) and TNF-α (Ct = 36.15).

The GSH levels in brains of control mice were 1997.33 ± 226.65 nmol/g wet tissues (Table 2). Administration of GNPs of different sizes did not alter the brain GSH levels irrespective of the dose regimens (ANVOA F = 0.265, P = 0.981). The levels of MDA in control mice brain were 8.50 ± 1.49 nmol/g we tissue (Table 2). There was no significant change in the levels of brain MDA after GNPs treatment of various sizes and dose regimens (ANOVA F = 0.286, P = 0.976).

4. Discussion

The results of this study showed that only small sized GNPs (5 nm) significantly increased IL-1β and IL-6 genes expressions whereas the larger GNPs (20 nm and 50 nm) did not affect these cytokines expression in mouse brain (Fig. 3). Microglial cells or microglia are the resident immune cells in the brain that are primarily involved in surveillance, macrophagy, production of cytokines and neurotrophic factors. Hutter et al. (2010) have demonstrated that GNP morphology (size and shape) as well as surface chemistry strongly influence the microglial activation after GNPs exposure, both in-vivo and in-vitro. Administration of GNPs directly into the rat brain (intracerebral injection) showed that small sized GNPs (5 nm) caused more nestin (an intermediate neurofilament protein) expression as compared to large sized (100 nm) GNPs (Lee et al., 2016). In a rat model of glioma, 1.9 nm GNPs were found to be toxic following intracerebral injection whereas no toxicity was observed using 15 nm GNPs at the same concentration (Bobyk et al., 2013). After inhalation exposure, smaller GNPs
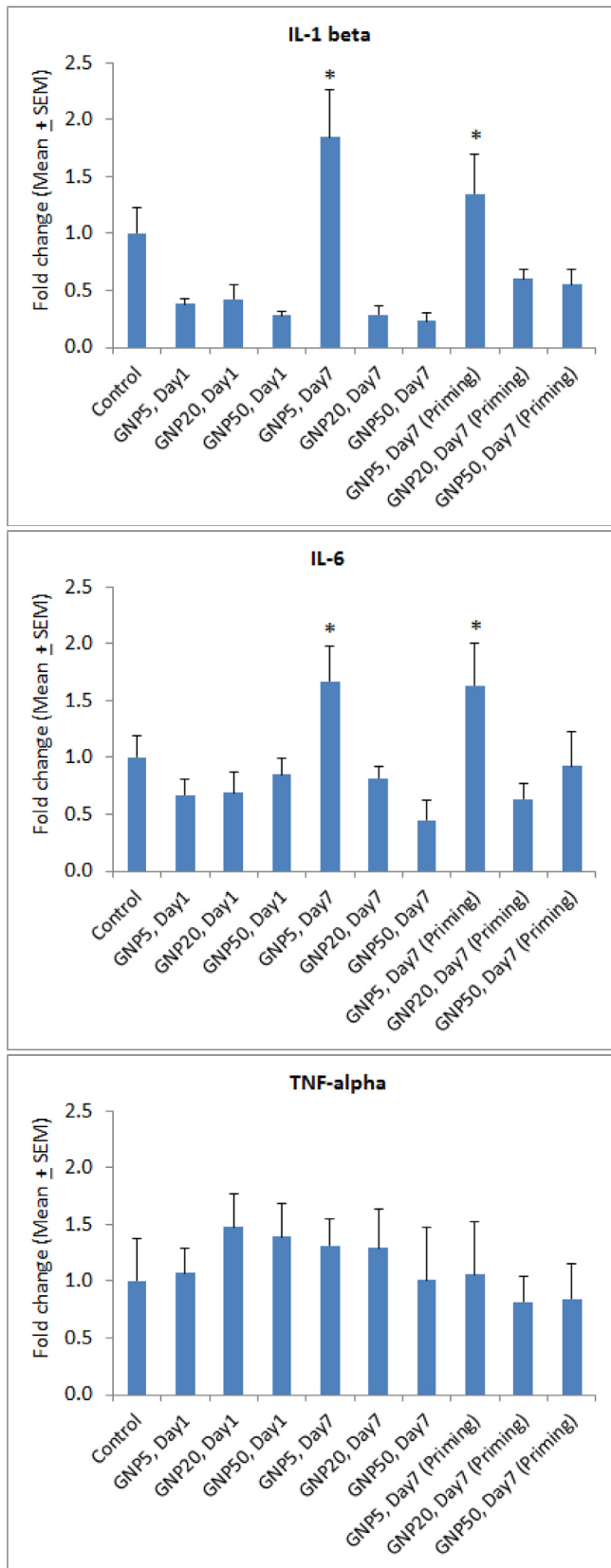
Fig. 3. Effect of GNPs on IL-1β, IL-6 and TNF-α mRNA expression in mice brain.
*P < 0.05 versus control group using Dunnett's multiple comparison test.

(13 nm) were able to translocate from the lungs to extrapulmonary organs at a faster rate than the larger GNPs (105 nm); although the small GNPs were found in liver, spleen, brain, testes and blood, the large GNPs were only detected in blood (Han et al., 2015). In a rat model of cerebral ischemic reperfusion injury, administration of 20 nm GNPs significantly inhibited the activation of astrocytes and microglia and elevated the production of anti-inflammatory cytokines resulting in remarkable amelioration of neurologic deficits and infarction volumes (Liu et al., 2013). On the other hand, small sized GNPs (5 nm) exerted opposite effects indicating an important role of GNPs size on modulating inflammatory and apoptotic mediators. Intraperitoneal injection of GNPs (0.5–15 mg/kg) showed that 17 nm GNPs crossed BBB more rapidly than 37 nm GNPs while both the GNPs significantly altered dopamine and serotonin levels in mice brain (Chen et al., 2010). Microscopic examination revealed that only small size GNPs (17 nm) entered the hippocampal region and impaired the cognitive function in mice (Chen et al., 2010).

There was no change in mRNA expression of proinflammatory cytokines on day 1 post-dosing of GNPs whereas a significant increase in IL-1β and IL-6 expression was observed on day 7 (Fig. 3). Previous reports have shown that, in liver and kidneys or rats, GNPs administration caused significant increase on day 1 which was receded on day 7 (Khan et al., 2013a, 2013b). The delayed induction of inflammatory response in brain as compared to liver and kidneys can be linked to variable bio-distribution of GNPs in different organs. After a single intravenous injection of GNPs (10, 50, 100 and 250 nm), their tissue distribution was found to be size-dependent with the smallest 10 nm GNPs showed the most widespread organ distribution including blood, liver, spleen, kidney, testis, thymus, heart, lung and brain, whereas the larger particles were only detected in blood, liver and spleen (De Jong et al., 2008). Takeuchi et al (Takeuchi et al., 2017) studied the biodistribution profile of GNPs of various particle sizes (20, 50 and 100 nm) and found that especially 20 nm GNPs were accumulated in lung and brain after 2–3 h of intravenous injection and they were retained for 24 h. Biokinetics of ultrafine GNPs (2, 5 and 10 nm) after a single intravenous administration of 1250 µg/kg dose in mice showed highest accumulation of gold in spleen on day 15 whereas a low concentration was detected in brain on day 1 without any residual GNPs after 30 days (Naz et al., 2016). After a single intravenous injection in mice, GNPs (15 and 50 nm) were able to pass BBB as evident from gold concentration in brain, measured by inductively coupled plasma mass spectrometry analysis (Sonavane et al., 2008). There is also an important role of particle size in immune response because of the variable deposition of complement proteins which is influenced by the nanoparticle size. Complement system significantly affects the uptake and clearance of NPs as well as the modulation of proinflammatory immune response (Pondman et al., 2015).

The second dose of GNPs (primed groups) did not show any cumulative effect of GNP doses on induction of proinflammatory cytokines in brain (Fig. 3). In rats, repeated intraperitoneal injections of 20 nm GNPs for 21 days showed similar levels of gold in brain and liver (Muller et al., 2017). Lasagna-Reeves et al. (2010) evaluated the bioaccumulation and toxic effects of different doses (40, 200, and 400 µg/kg) of 12.5 nm GNPs after daily intraperitoneal injections in mice for 8 days. Their findings showed that GNPs crossed the BBB and accumulated in the neural tissue although their accumulation was least in brain as compared to other organs. However, the repeated exposure of GNPs did not produce any sub-acute physiological damage and toxicity in terms of survival, behavior, animal weight, organ morphology, blood biochemistry and tissue histology (Lasagna-Reeves et al., 2010). The priming dose of GNPs protected the animals against the acute phase induction of proinflammatory cytokines in liver and spleen (Ibrahim et al., 2018b). The primed mice did not show any aggravation of histological changes after injecting the second dose of the same GNPs (Ibrahim et al., 2018a).

Amplification curves

Melting curves

IL-1β

IL-6

TNF-α
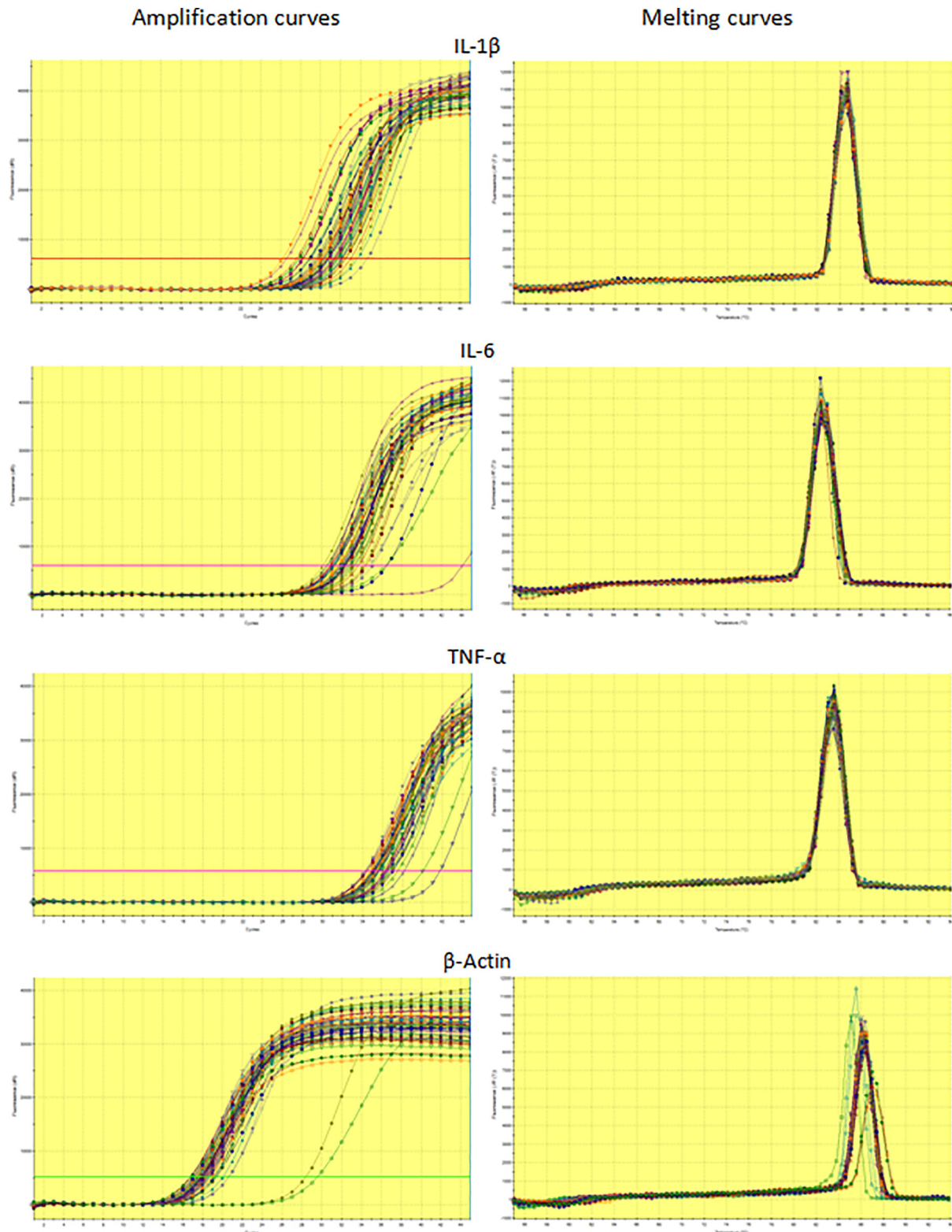
β-Actin

Fig. 4. Real-time PCR amplification curves (left panel) and melting curves (right panel) for target (IL-1β, IL-6, TNF-α) and house-keeping (β-Actin) genes expressions.

We did not observe any significant change in brain levels of GSH and MDA following GNPs exposure, irrespective of their sizes (Table 2). In a previous study, intraperitoneal administration of 20 nm GNPs in rats for 21 days did not alter GSH levels as well as the activities of superoxide dismutase (SOD), glutathione perox-idase (GPx), and catalase (CAT), in brain samples (Muller et al., 2017). Ferreira et al. (2017) observed a decrease in thiobarbituric acid-reactive species (TBARS) after acute (single dose) intraperi-toneal administration of GNPs (10 nm and 30 nm, 70 μg/kg) whereas the activity of SOD was increased after acute and long-term (28 days) exposure of GNPs in rats. Intraperitoneal injection of 10 nm GNPs significantly increased MDA in rat liver without

Table 2
Effect of GNPs on GSH and MDA levels in mouse brain.

Treatment group	GSH (nmol/g)	MDA (nmol/g)
Control	1997.33 ± 226.65	8.50 ± 1.49
GNP 5 nm (day 1)	2003.50 ± 200.36	8.57 ± 1.48
GNP 20 nm (day 1)	1923.00 ± 167.84	8.49 ± 1.53
GNP 50 nm (day 1)	1861.75 ± 206.29	7.10 ± 1.17
GNP 5 nm (day 7)	2013.75 ± 264.91	8.00 ± 1.62
GNP 20 nm (day 7)	1739.91 ± 160.31	6.23 ± 1.18
GNP 50 nm (day 7)	1794.60 ± 194.72	8.44 ± 2.63
GNP 5 nm (day 1, 7)	1933.25 ± 167.91	7.30 ± 1.18
GNP 20 nm (day 1, 7)	2064.41 ± 190.01	7.01 ± 1.19
GNP 50 nm (day 1, 7)	1960.16 ± 176.27	7.25 ± 1.38

Values are mean ± standard error.

altering GSH levels on days 3 and 7 (Khan et al., 2012). In a rat model of Alzheimer's disease, GNP treatment not only reversed the streptozotocin-induced impairment in mitochondrial ATP production, neuroinflammation and oxidative stress but also prevented memory deficits (Muller et al., 2017). Hyun et al. (2013) have used fluorescein-labeled hyaluronic acid-immobilized GNPs for monitoring ROS level in the ischemic brain and to identify the infarct areas in ischemic brains for the treatment of stroke. The findings of our study about the inertness of GNPs in affecting the markers of oxidative stress strengthen their usefulness in developing sensors for determining ROS levels in neuronal tissues.

5. Conclusion

A single intraperitoneal injection of small sized GNPs (5 nm) significantly increased IL-1β and IL-6 mRNA expressions in mouse brain which was not exacerbated by the second dose of the same GNPs. The larger size GNPs (20 and 50 nm) did not produce any inflammatory response in mouse brain. The findings of this study have potential relevance in designing new strategies for GNP applications in imaging and therapy of neurological disorders.

Acknowledgments

References

Betzer, O., Shilo, M., Opochinsky, R., Barnoy, E., Motiei, M., Okun, E., Yadid, G., Popovtzer, R., 2017. The effect of nanoparticle size on the ability to cross the blood-brain barrier: an in vivo study. Nanomedicine (Lond). 12, 1533–1546.

Bobyk, L., Edouard, M., Deman, P., Vautrin, M., Pernet-Gallay, K., Delaroche, J., Adam, J.F., Estève, F., Ravanat, J.L., Elleaume, H., 2013. Photoactivation of gold nanoparticles for glioma treatment. Nanomedicine 9, 1089–1097.

Cabezón, I., Manich, G., Martín-Venegas, R., Camins, A., Pelegrí, C., Vilaplana, J., 2015. Trafficking of gold nanoparticles coated with the 8D3 anti-transferrin receptor antibody at the mouse blood-brain barrier. Mol. Pharm. 12, 4137–4145.

Calderón-Gonzalez, R., Terán-Navarro, H., Frande-Cabanes, E., et al., 2016. Pregnancy vaccination with gold glyco-nanoparticles carrying Listeria monocytogenes peptides protects against listeriosis and brain- and cutaneous-associated morbidities. Biomaterials (Basel) 6, pii: E151.

Chen, Y.S., Hung, Y.C., Lin, L.W., Liau, I., Hong, M.Y., Huang, G.S., 2010. Size-dependent impairment of cognition in mice caused by the injection of gold nanoparticles. Nanotechnology 21, 485102.

Cheng, Y., Dai, Q., Morshed, R.A., et al., 2014. Blood-brain barrier permeable gold nanoparticles: an efficient delivery platform for enhanced malignant glioma therapy and imaging. Small 10, 5137–5150.

Chithrani, B.D., Chan, W.C., 2007. Elucidating the mechanism of cellular uptake and removal of protein-coated gold nanoparticles of different sizes and shapes. Nano Lett. 7, 1542–1550.

De Jong, W.H., Hagens, W.I., Krystek, P., Burger, M.C., Sips, A.J., Geertsma, R.E., 2008. Particle size-dependent organ distribution of gold nanoparticles after intravenous administration. Biomaterials 29, 1912–1919.

Eswar, K.A., Rouhi, J., Husairi, F.S., Dalvand, R., Alrokayan, S.A., Khan, H.A., Mahmood, R., Abdullah, S., 2014. Hydrothermal growth of flower-like ZnO nanostructures on porous silicon substrate. J. Mol. Struct. 1074, 140–143.

Falagan-Lotsch, P., Grzincic, E.M., Murphy, C.J., 2016. One low-dose exposure of gold nanoparticles induces long-term changes in human cells. PNAS 113, 13318–13323.

Ferreira, G.K., Cardoso, E., Vuolo, F.S., et al., 2017. Effect of acute and long-term administration of gold nanoparticles on biochemical parameters in rat brain. Mater. Sci. Eng. C Mater. Biol. Appl. 79, 748–755.

Guerrero, S., Araya, E., Fiedler, J.L., Arias, J.I., Adura, C., Albericio, F., Giralt, E., Arias, J.L., Fernández, M.S., Kogan, M.J., 2010. Improving the brain delivery of gold nanoparticles by conjugation with an amphipathic peptide. Nanomedicine (Lond). 5, 897–913.

Hainfeld, J.F., Smilowitz, H.M., O'Connor, M.J., Dilmanian, F.A., Slatkin, D.N., 2013. Gold nanoparticle imaging and radiotherapy of brain tumors in mice. Nanomedicine (Lond). 8, 1601–1609.

Han, S.G., Lee, J.S., Ahn, K., et al., 2015. Size-dependent clearance of gold nanoparticles from lungs of Sprague-Dawley rats after short-term inhalation exposure. Arch. Toxicol. 89, 1083–1094.

Hutter, E., Boridy, S., Labrecque, S., Lalancette-Hébert, M., Kriz, J., Winnik, F.M., Maysinger, D., 2010. Microglial response to gold nanoparticles. ACS Nano 4, 2595–2606.

Hyun, H., Lee, K., Min, K.H., Jeon, P., Kim, K., Jeong, S.Y., Kwon, I.C., Park, T.G., Lee, M., 2013. Ischemic brain imaging using fluorescent gold nanoprobes sensitive to reactive oxygen species. J. Control. Release 170, 352–357.

Ibrahim, K.E., Al-Mutary, M.G., Bakhiet, A.O., Khan, H.A., 2018a. Histopathology of the liver, kidney, and spleen of mice exposed to gold nanoparticles. Molecules 23 (8), pii: E1848.

Ibrahim, K.E., Bakhiet, A.O., Awadalla, M.E., Khan, H.A., 2018b. A priming dose protects against gold nanoparticles-induced proinflammatory cytokines mRNA expression in mice. Nanomedicine (Lond). 13, 313–323.

Kang, S.H., Nafiujjaman, M., Nurunnabi, M., Li, L., Khan, H.A., Cho, K.J., Huh, K.M., Lee, Y., 2015. Hybrid photoactive nanomaterial composed of gold nanoparticles, pheophorbide-A and hyaluronic acid as a targeted bimodal phototherapy. Macromol. Res. 23, 474–484.

Khan, H.A., Abdelhalim, M.A., Al-Ayed, M.S., Alhomida, A.S., 2012. Effect of gold nanoparticles on glutathione and malondialdehyde levels in liver, lung and heart of rats. Saudi J. Biol. Sci. 19, 461–464.

Khan, H.A., Abdelhalim, M.A., Alhomida, A.S., Al-Ayed, M.S., 2013a. Effects of naked gold nanoparticles on proinflammatory cytokines mRNA expression in rat liver and kidney. Biomed. Res. Int. 2013, 590730.

Khan, H.A., Abdelhalim, M.A., Alhomida, A.S., Al Ayed, M.S., 2013b. Transient increase in IL-1β, IL-6 and TNF-α gene expression in rat liver exposed to gold nanoparticles. Genet. Mol. Res. 12, 5851–5857.

Khan, H.A., Shanker, R., 2015. Toxicity of nanomaterials. Biomed. Res. Int. 2015, 521014.

Khan, H.A., Ibrahim, K.E., Khan, A., Alrokayan, S.H., Alhomida, A.S., 2017. Immunostaining of proinflammatory cytokines in renal cortex and medulla of rats exposed to gold nanoparticles. Histol. Histopathol. 32, 597–607.

Khan, H.A., Ibrahim, K.E., Khan, A., Alrokayan, S.H., Alhomida, A.S., Lee, Y.K., 2016. Comparative evaluation of immunohistochemistry and real-time PCR for measuring proinflammatory cytokines gene expression in livers of rats treated with gold nanoparticles. Exp. Toxicol. Pathol. 68, 381–390.

Khatun, Z., Nurunnabi, M., Nafiujjaman, M., Reeck, G.R., Khan, H.A., Cho, K.J., Lee, Y.K., 2015. A hyaluronic acid nanogel for photo-chemo theranostics of lung cancer with simultaneous light-responsive controlled release of doxorubicin. Nanoscale 7, 10680–10689.

Lasagna-Reeves, C., Gonzalez-Romero, D., Barria, M.A., Olmedo, I., Clos, A., Sadagopa Ramanujam, V.M., Urayama, A., Vergara, L., Kogan, M.J., Soto, C., 2010. Bioaccumulation and toxicity of gold nanoparticles after repeated administration in mice. Biochem. Biophys. Res. Commun. 393, 649–655.

Lee, U., Yoo, C.J., Kim, Y.J., Yoo, Y.M., 2016. Cytotoxicity of gold nanoparticles in human neural precursor cells and rat cerebral cortex. J. Biosci. Bioeng. 121, 341–344.

Li, C.H., Shyu, M.K., Jhan, C., et al., 2015. Gold nanoparticles increase endothelial paracellular permeability by altering components of endothelial tight junctions, and increase blood-brain barrier permeability in mice. Toxicol. Sci. 148, 192–203.

Liu, Z., Shen, Y., Wu, Y., Yang, Y., Wu, J., Zhou, P., Lu, X., Guo, Z., 2013. An intrinsic therapy of gold nanoparticles in focal cerebral ischemia-reperfusion injury in rats. J. Biomed. Nanotechnol. 9, 1017–1028.

Meyers, J.D., Cheng, Y., Broome, A.M., et al., 2015. Peptide-targeted gold nanoparticles for photodynamic therapy of brain cancer. Part. Part. Syst. Char. 32, 448–457.

Miladi, I., Alric, C., Dufort, S., et al., 2014. The in vivo radiosensitizing effect of gold nanoparticles based MRI contrast agents. Small 10, 1116–1124.

Muller, A.P., Ferreira, G.K., Pires, A.J., de Bem, Silveira G, de Souza, D.L., Brandolfi, J.A., de Souza, C.T., Paula, M.M.S., Silveira, P.C.L., 2017. Gold nanoparticles prevent cognitive deficits, oxidative stress and inflammation in a rat model of sporadic dementia of Alzheimer's type. Mater. Sci. Eng. C Mater. Biol. Appl. 77, 476–483.

Muller, A.P., Ferreira, G.K., da Silva, S., Nesi, R.T., de Bem, Silveira G, Mendes, C., Pinho, R.A., da Silva Paula, M.M., Silveira, P.C.L., 2017. Safety protocol for the gold nanoparticles administration in rats. Mater. Sci. Eng. C Mater. Biol. Appl. 77, 1145–1150.

Nafiujjaman, M., Nurunnabi, M., Kang, S.H., Reeck, G., Khan, H.A., Lee, Y.K., 2015. Ternary graphene quantum dot-polydopamine-Mn3O4 nanoparticles for optical imaging guided photodynamic therapy and T1-weighted magnetic resonance imaging. J. Mater. Chem. B 3, 5815–5823.

Nafiujjaman, M., Khan, H.A., Lee, Y.K., 2017. Peptide-influenced graphene quantum dots on iron oxide nanoparticles for dual imaging of lung cancer cells. J. Nanosci. Nanotech. 17, 1704–1711.

Naz, F., Koul, V., Srivastava, A., Gupta, Y.K., Dinda, A.K., 2016. Biokinetics of ultrafine gold nanoparticles (AuNPs) relating to redistribution and urinary excretion: a long-term in vivo study. J. Drug Target. 24, 720–729.

Nurunnabi, M., Parvez, K., Nafiujjaman, M., Revuri, V., Khan, H.A., Feng, X., Lee, Y., 2015. Bioapplication of graphene oxide derivatives: drug/gene delivery, imaging, polymeric modification, toxicology, therapeutics and challenges. RSC Adv. 5, 42141–42161.

Pondman, K.M., Pednekar, L., Paudyal, B., Tsolaki, A.G., Kouser, L., Khan, H.A., Shamji, M.H., Haken, B.T., Stenbeck, G., Sim, R.B., Kishore, U., 2015. Innate immune humoral factors, C1q and factor H, with differential pattern recognition properties, alter macrophage response to carbon nanotubes. Nanomedicine 11, 2109–2118.

Prades, R., Guerrero, S., Araya, E., Molina, C., Salas, E., Zurita, E., Selva, J., Egea, G., López-Iglesias, C., Teixidó, M., Kogan, M.J., Giralt, E., 2012. Delivery of gold nanoparticles to the brain by conjugation with a peptide that recognizes the transferrin receptor. Biomaterials 33, 7194–7205.

Ruan, S., Yuan, M., Zhang, L., et al., 2015. Tumor microenvironment sensitive doxorubicin delivery and release to glioma using angiopep-2 decorated gold nanoparticles. Biomaterials 37, 425–435.

Salifairus, M.J., Hamid, S.B.A., Soga, T., Alrokayan, S.A.H., Khan, H.A., Rusop, M., 2016. Structural and optical properties of graphene from green carbon source via thermal chemical vapor deposition. J. Mat. Res. 31, 1947–1956.

Sonavane, G., Tomoda, K., Makino, K., 2008. Biodistribution of colloidal gold nanoparticles after intravenous administration: effect of particle size. Colloids Surf. B Biointerfaces 66, 274–280.

Takeuchi, I., Nobata, S., Oiri, N., Tomoda, K., Makino, K., 2017. Biodistribution and excretion of colloidal gold nanoparticles after intravenous injection: effects of particle size. Biomed. Mater. Eng. 28, 315–323.

Zhang, Y., Walker, J.B., Minic, Z., Liu, F., Goshgarian, H., Mao, G., 2016. Transporter protein and drug-conjugated gold nanoparticles capable of bypassing the blood-brain barrier. Sci. Rep. 6, 25794.